JACS
JOURNAL OF THE AMERICAN CHEMICAL SOCIETY
Communication
pubs.acs.org/JACS

Carrier Concentration Dependent Conduction in Insulator-Doped Donor/Acceptor Chain Compounds

Masaki Nishio,[†] Norihisa Hoshino,[‡] Wataru Kosaka,[§] Tomoyuki Akutagawa,[‡] and Hitoshi Miyasaka*[,§]

[†]Department of Chemistry, Division of Material Sciences, Graduate School of Natural Science and Technology, Kanazawa University, Kakuma-machi, Kanazawa 920-1192, Japan

[‡]Institute of Multidisciplinary Research for Advanced Materials, Tohoku University, 2-1-1 Katahira, Aoba-ku, Sendai 980-8577, Japan

[§]Institute for Materials Research, Tohoku University, 2-1-1 Katahira, Aoba-ku, Sendai 980-8577, Japan

Supporting Information

ABSTRACT: On the basis of the concept that the design of a mixed valence system is a key route to create electronic conducting frameworks, we propose a unique idea to rationally produce mixed valency in an ionic donor/acceptor chain (i.e., D^+A^- chain). The doping of a redox-inert (insulator) dopant (P) into a D^+A^- chain in place of neutral D enables the creation of mixed valency A^0/A^- domains between P units: $P-(D^+A^-)_nA^0-P$, where n is directly dependent on the dopant ratio, and charge transfer through the P units leads to electron transport along the framework. This hypothesis was experimentally demonstrated in an ionic DA chain synthesized from a redox-active paddlewheel $[Ru_2^{II,II}]$ complex and TCNQ derivative by doping with a redox-inert $[Rh_2^{II,II}]$ complex.

The design of electronically conducting materials is a longstanding theme in the field of molecular functional materials. In particular, attaining it using low-dimensional covalently bonded or coordinating frameworks (i.e., charge transfer metal−organic frameworks, CTMOFs) remains a big challenge. To date, only a few families of highly conducting one-dimensional chain compounds have been identified,[1,2] e.g., Krogmann salts (or KCP derivatives) such as $K_2[Pt(CN)_4]$-$Br_{0.3}\cdot 3H_2O$,[3] partially oxidized oxalate Pt complexes such as $K_{1.62}[Pt(C_2O_4)_2]\cdot 2H_2O$,[4] halogenocarbonyl Ir complexes such as $[Ir(CO)_3Cl]$,[5] metal wire complexes,[6−8] and halogen-bridged metal complexes.[9−11] All these compounds are mixed valence metal systems, synthesized mainly by one of the following techniques: partial chemical oxidation in assembly reaction media with an adequate oxidant such as halogen (chemical oxidation method), crystallization from a non-stoichiometric mixture of different valence precursors (substitutional doping method), or electrochemical syntheses (electrochemical oxidation method). Thus, a key way to design conducting CTMOFs is the construction of continuous mixed valency in a framework; however, the development of novel methodology to rationally obtain mixed valence frameworks is an important issue in this research area.

Here we propose a new idea to create mixed valency in a chain to systematically enable the tuning of charge carrier density, focusing on a family of one-dimensional chains composed of electron donors (D) and electron acceptors (A), i.e., DA chains (Figure 1a), followed by electron transfer to form an ionic DA chain (i.e., D^+A^- chain; Figure 1b). Now we consider a redox-inert dummy unit (P as a means of "pinning"), which can partially replace D units in a DA chain. If the redox-inert P units are doped into a neutral DA chain to form a $D_{(1-x)}P_xA$ chain (Figure 1c), followed by electron transfer D→A, the doped ionic chain should have A^0/A^- domains between P units independent of the size of domains (Figure 1d). Note that we call finite chains isolated by two P units "domains," and the mixed valency in domains is given by the A^0/A^- sets. Therefore, the A^0/A^- pair can move within a domain, creating a charge dynamical domain. Thus, the number of A^0/A^- sets is equal to the number of domains, which is dependent on the doping level. There are four possible charge arrangements for adjacent A units around P, as depicted in Figure 1e−1h. Importantly, if the dopant P completely cuts off the communication (i.e., exchange of charge) between domains, the motion of an A^0/A^- set within a domain is merely an exchange of dipoles ($A^0A^-\leftrightarrow A^-A^0$), which may be detectable as a permittivity response (electron-pinned defect dipoles),[12] whereas if any electronic interaction is possible through the dopant P, charge transport beyond a domain would be permitted. Hence, the doping of redox-inert P units into ionic DA chains rationally produces mixed valency in the system, and if the energy barrier at P is not high, i.e., with a tunneling electron transfer between A^0PA^- and A^-PA^0 states (Figure 1f and 1g), the electronic conductance in the chain could be mainly dependent on the charge carrier concentration (i.e., the number of the A^0/A^- set) proportional to the amount of dopant P.

To experimentally prove this hypothesis, we synthesized a DA chain: $[Ru_2(2\text{-MeO-4-ClPhCO}_2)_4(BTDA\text{-TCNQ})]\cdot 2.5(benzene)$ (**1**), in which the donor is the paddlewheel-type diruthenium(II, II) complex $[Ru_2^{II,II}(2\text{-MeO-4-ClPhCO}_2)_4]$ (2-MeO-4-$ClPhCO_2^-$ = 2-methoxy-4-chlorobenzoate) and the acceptor is BTDA-TCNQ (= bis(1,2,5-thiadiazolo)tetracyanoquinodimethane) (Supporting Information). Note that this D/A combination was chosen for its potential to exist in ionic form according to an ionicity diagram from related materials.[13,14] In fact, the energy gap estimated by DFT calculations between the HOMO level of $[Ru_2^{II,II}(2\text{-MeO-4-ClPhCO}_2)_4(THF)_2]$ (−4.1323 eV) and the LUMO level of

Received: September 21, 2013
Published: October 28, 2013

ACS Publications © 2013 American Chemical Society

dx.doi.org/10.1021/ja409785a | J. Am. Chem. Soc. 2013, 135, 17715−17718

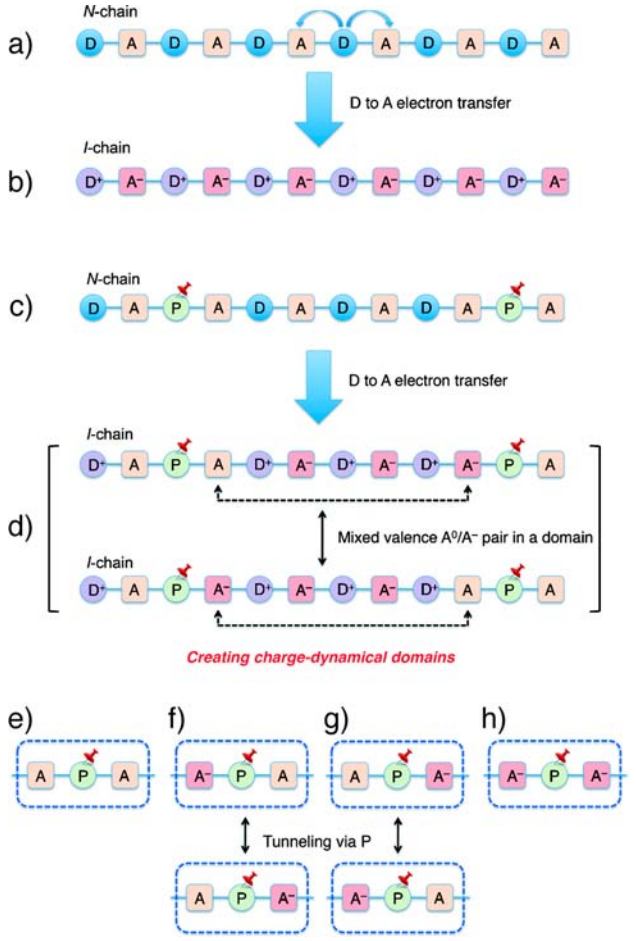

Figure 1. Schematic representations of charge arrangements possibly found in DA chains and P-doped DA chains derived by electron transfer from D to A, where P (as "pinning") is a redox-inert dopant. (a) Regular neutral DA chain. (b) Regular ionic DA chain (i.e., regular D^+A^- chain). (c) P-doped neutral DA chain. (d) P-doped ionic DA chain, which forms degenerate mixed-valence states $[(D^+A^-)_nA^0]$ between P units independent of the size of domains. (e–h) Four possible states around the P unit, (f) and (g) being interchangeable if an electron/hole transfer through the P unit is possible.

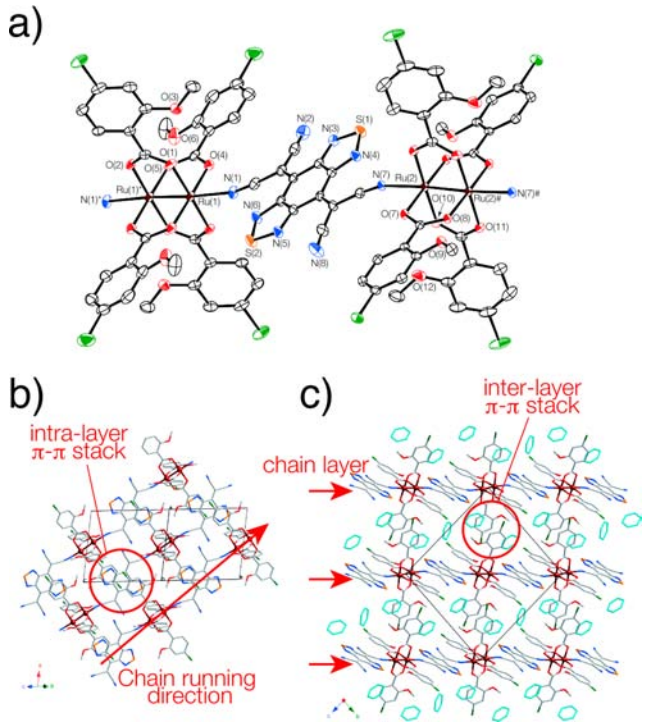

Figure 2. Crystal structure of **1**. (a) Ortep drawing of the asymmetric unit (50% probability ellipsoids; symmetry: *, $-x-1, -y+1, -z+1$; #, $-x+1, -y+2, -z$). (b) A packing diagram projected along the ⟨011⟩ direction, representing a "chain layer" (the (011) plane). (c) A packing diagram projected along the *a* axis, i.e., along the layer, where the benzene molecules as interstitial solvents are shown in pale blue color. The red circles indicate areas of $\pi-\pi$ stacking. Hydrogen atoms were omitted for clarity.

BTDA-TCNQ (−4.7353 eV) is significantly large, at −0.603 eV (Supporting Information).

Compound **1** crystallized in the triclinic $P\bar{1}$ space group with $Z = 2$ (Figure 2; Table S1). Although BTDA-TCNQ could act as a tetradentate ligand with four cyano groups,[14d,e,g] the moiety in **1** acted as a linear-type bidentate ligand using only two cyano groups in a *trans* position, forming a DA alternating chain similar to chain compounds based on *N*,*N*′-dicyanoquinodiimine (DCNQI).[14h] The repeating unit can be described as a half of [−{$Ru(1)_2$}−(BTDA-TCNQ)−{$Ru(2)_2$}−(BTDA-TCNQ)−] (Figure 2a). Compound **1** is an ionic chain, and the charge distribution in D^+A^- is constant over the temperature range below 300 K as proved by structural comparison (see Supporting Information; Tables S2 and S3) and magnetic properties that reveal a ferrimagnetic spin arrangement with $S = 3/2$ for $[Ru_2^{II,III}]^+$ and $S = 1/2$ for BTDA-TCNQ$^{\bullet-}$ (Supporting Information; Figure S1). The chains run along the ⟨21−1⟩ direction to form a chain-aggregated layer on the (011) plane (hereafter called a "chain layer"; see Figure 2b and 2c). In this chain layer, chains are closely packed in an antiphase manner with interchain $\pi-\pi$ stacking between the 2-MeO-4-Cl-Ph group of $[Ru_2]$ and BTDA-TCNQ, resulting in relatively short $[Ru_2]$···BTDA-TCNQ distances of ca. 7.2 Å (Figure S2). On the other hand, the crystallization solvents (2.5 molecules of benzene) are present between the chain layers (Figure 2b); thus, chains, aligning in an in-phase manner along the ⟨011⟩ direction, are significantly separated by ca. 12 Å (Figure S2), although $\pi-\pi$ stacking between benzoate groups occurs (Figure 2b).

The Rh-derivative of **1**, $[Rh_2(2\text{-MeO-4-ClPhCO}_2)_4(\text{BTDA-TCNQ})]\cdot 2.5(\text{benzene})$ (**1-Rh**), with its P-only chain, was also synthesized as a reference (Supporting Information), isostructural to **1** as confirmed by single-crystal X-ray crystallography (Figure S3; Tables S1–S3). The $[Rh_2^{II,II}(2\text{-MeO-4-ClPhCO}_2)_4]$ unit ($[Rh_2^{II,II}]$) is redox-inert; thus, the BTDA-TCNQ moiety is neutral (Table S3). Thereafter, the $[Rh_2^{II,II}]$ unit was doped into **1** at 3.3, 5.0, and 20 mol %, where the actual dopant composition analyzed by ICP-MS is close to the added amount in the syntheses: $[\{(Ru_2)_{1-x}(Rh_2)_x(2\text{-MeO-4-ClPhCO}_2)_4\}(\text{BTDA-TCNQ})]\cdot 2.5(\text{benzene})$ ($x = 0.03$, **Rh-3%**; 0.05, **Rh-5%**; 0.16, **Rh-16%**). The doped compounds were structurally characterized and confirmed to be isostructural to **1** (Tables S1–S3). The comparison of bond lengths in this series proved that the $[Rh_2^{II,II}]$ unit was present at the estimated dopant rate *x* (Figure S4). Furthermore, to establish whether $[Rh_2^{II,II}]$ units truly replaced $[Ru_2]$ units in **1** rather than existing in a mixture of separate **1** and **1-Rh** crystals, X-ray fluorescence analysis was performed for each single crystal and characteristic Rh peaks were quantitatively detected dependent on *x* (Figure S5). Thus, the target $[Rh_2]$-doped compounds

dx.doi.org/10.1021/ja409785a | J. Am. Chem. Soc. 2013, 135, 17715–17718

were successfully synthesized, as illustrated in Figure 1d, although their absorption spectra are almost identical to those of **1** (Figure S6).

Figure 3a shows the dc resistivity (ρ_{dc}) of all compounds (except insulating **1-Rh**) as a function of temperature measured

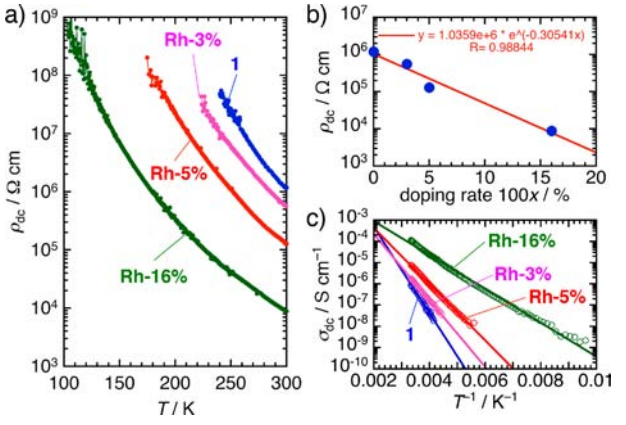

Figure 3. (a) Temperature dependence of ρ_{dc} measured on single crystals of **1**, **Rh-3%**, **Rh-5%**, and **Rh-16%** by two-probe dc-current technique. (b) Variation of ρ_{dc} at 300 K with the doping rate 100x, where the red line represents a fitting line by an exponential function noted in the figure. (c) Arrhenius plots of σ_{dc}. The activation energy (E_a(dc)) is listed in Table 1.

by a two-probe dc-current technique on single crystals (parallel to the chain). All compounds exhibit typical semiconductor behavior, but ρ_{dc} tends to decrease exponentially with increasing amount of [$Rh_2^{II,II}$] dopant (Figure 3b): 1.2 × 10^6, 5.5 × 10^5, 1.3 × 10^5, and 8.8 × 10^3 Ω cm at 300 K for **1**, **Rh-3%**, **Rh-5%**, and **Rh-16%**, respectively (σ_{dc} = 8.4 × 10^{-7}, 1.8 × 10^{-6}, 7.8 × 10^{-6}, and 1.1 × 10^{-4} S cm^{-1}, respectively). The activation energy (E_a(dc)) estimated from Arrhenius plots (Figure 3c) is listed in Table 1. The ρ value of **Rh-16%** is

Table 1. Activation Energy Evaluated by dc (E_a(dc)) and ac (E_a(ac)) Electronic Techniques (Two Probe Method)

compd	E_a(dc)/meV	E_a(ac)/meV
1	403	
Rh-3%	310	201
Rh-5%	262	225
Rh-16%	158	197
1-Rh	–	–

smaller than that of **1** by more than 2 orders of magnitude. Considering the fact that the [$Rh_2^{II,II}$] unit is relatively redox-inert and **1-Rh** is an insulator (ρ_{dc} > 10^{10} Ω cm), the [$Rh_2^{II,II}$] unit itself cannot contribute as a carrier. Therefore, the charge carriers must be provided from the mixed valence A^0/A^- sets in domains with transfer through the [$Rh_2^{II,II}$] (P) units. To confirm the carrier type (electrons/holes or ions), time-dependent dc resistivity was measured at 250−300 K (0.2 s per a point) (Figure S7). Given the consistency of the ρ_{dc} value at each temperature and lack of time-dependency, electron/hole carriers are indicated. The activation energy E_a(dc) also decreased with increasing doping amount of the [$Rh_2^{II,II}$] unit, suggesting the electronic band structure changed with doping. However, the structure of the conducting pathway is essentially invariant, and the dopant P does not provide any energetically relevant electron/hole band. Thus, this electron transport should be dominated by the charge carrier density, i.e., the number of A^0/A^- sets. Consequently, E_a(dc) should be the activation energy for bulk conductivity. This mechanism is obvious according to the following ac impedance data.

Ac impedance spectra of single crystals examined the conducting behavior of these doped compounds. Figure 4

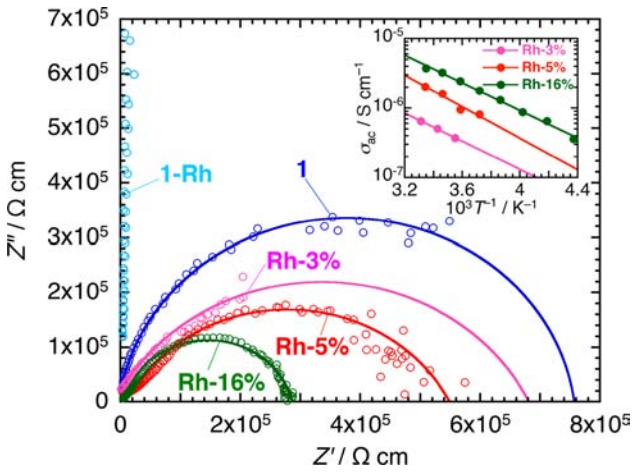

Figure 4. Nyquist plots for **1** (β = 0.95), **Rh-3%** (β = 0.72), **Rh-5%** (β = 0.71), **Rh-16%** (β = 0.86), and **1-Rh** at 300 K and their simulation curves based on a generalized Debye equation with β values. Inset: Arrhenius plots of σ_{ac} of **Rh-3%**, **Rh-5%**, and **Rh-16%** estimated from Nyquist plots measured at several temperatures. The activation energy (E_a(ac)) is listed in Table 1.

shows the Nyquist plots for **1**, **Rh-3%**, **Rh-5%**, **Rh-16%**, and **1-Rh** at 300 K and their simulation curves based on a generalized Debye equation $Z(\omega) = R_b/\{1 + (i\omega\tau)^{\beta}\}$ with β = 0.71−0.95 (Z = impedance; R_b = sample resistance; Debye relaxation as β = 1).[15] These semicircular plots prove that the electron conducting behavior is attributed to a single electron/hole hopping process, and the degree of conductance shows the order **1** < **Rh-3%** < **Rh-5%** < **Rh-16%**, consistent with the dc measurement results. The estimated ρ_{ac} value from the resistance R at 300 K ($\rho_{ac@300K}$) is as follows: 7.6 × 10^5, 6.8 × 10^5, 5.5 × 10^5, and 2.8 × 10^5 Ω cm, for **1**, **Rh-3%**, **Rh-5%**, and **Rh-16%**, respectively. Although $\rho_{ac@300K}$ of **Rh-16%** is slightly larger than $\rho_{dc@300K}$, the trend with x mirrors the dc measurement results. The inset of Figure 4 shows Arrhenius plots for σ_{ac} of **Rh-3%**, **Rh-5%**, and **Rh-16%**, and the estimated activation energies (E_a(ac)) are summarized together with E_a(dc) in Table 1. The important aspect is that the E_a(ac) values are almost invariant independent of x, and this trend conflicts with that in E_a(dc). Namely, dc conductivity is basically benefitted by increased numbers of carriers, and thus, the activation energy E_a(dc) reflects bulk conductance, whereas the ac conductance mainly describes the local conduction in the chain (i.e., the interdomain electron transfer), which is associated with the energy barrier to pass the P dopant. Hence, E_a(ac) reflects the intrinsic nature of the system involving the nature of P, and E_a(ac) ≈ 150−200 meV represents the essential activation energy for electron/hole hopping beyond the P units.

In conclusion, a novel ionic DA chain (i.e., D^+A^-) was synthesized using the highly redox-active [Ru_2(2-MeO-4-$ClPhCO_2)_4$] unit and BTDA-TCNQ, in which the doping of a "redox-inert" dopant [Rh_2] in place of [Ru_2] could enhance the electronic conductivity through the chain. This is probably

dx.doi.org/10.1021/ja409785a | J. Am. Chem. Soc. 2013, 135, 17715−17718

because of the formation of mixed valence of A^0/A^- in domains isolated by the dopant $[Rh_2]$ units followed by charge transfer through the dopant $[Rh_2]$ units. This mechanism provides a unique way to design CTMOFs.

■ ASSOCIATED CONTENT

Ⓢ Supporting Information

Experimental procedures for **1**, **1-Rh**, **Rh-3%**, **Rh-5%**, and **Rh-16%**, details of X-ray crystallography and structural data, Tables S1−S3, Figures S1−S7. This information is available free of charge via the Internet at http://pubs.acs.org.

■ AUTHOR INFORMATION

Corresponding Author

miyasaka@imr.tohoku.ac.jp

Notes

The authors declare no competing financial interest.

■ ACKNOWLEDGMENTS

The authors thank Dr. Kimiko Hasegawa at RIGAKU Co. Ltd. for measurements of X-ray fluorescent spectroscopy. This work was supported by a Grant-in-Aid for Scientific Research (Nos. 24245012, 25620041) and for Innovative Areas ("Coordination Programming" Area 2107, No. 24108714) from MEXT, Japan, the Sumitomo Foundation, and the Asahi Glass Foundation.

■ REFERENCES

(1) *Extended Linear Chain Compounds*, Vol. *I*; Miller, J. S., Ed.; Plenum Press: New York and London, 1982.

(2) Lecrone, F. N.; Minot, M. J.; Perlstein, J. H. *Inorg. Nucl. Chem. Lett.* **1972**, *8*, 173−179.

(3) Zeller, H. R.; Beck, A. *J. Phys. Chem. Solids* **1974**, *35*, 77−80.

(4) Kobayashi, A.; Sasaki, Y.; Shirotani, I.; Kobayashi, H. *Solid State Commun.* **1978**, *26*, 653−656.

(5) Ginsberg, A. P.; Koepke, J. W.; Hauser, J. J.; West, K. W.; Di Salvo, F. J.; Sprinkle, C. R.; Cohen, R. L. *Inorg. Chem.* **1976**, *15*, 514−519.

(6) (a) Prater, M. E.; Pence, L. E.; Clérac, R.; Finniss, G. M.; Campana, C.; Abban-Senzier, P.; Jérome, D.; Canadell, E.; Dunbar, K. R. *J. Am. Chem. Soc.* **1999**, *121*, 8005−8016. (b) Bera, J. K.; Dunbar, K. R. *Angew. Chem., Int. Ed.* **2002**, *41*, 4453−4457.

(7) Mitsumi, M.; Goto, H.; Umebayashi, S.; Ozawa, Y.; Kobayashi, M.; Yokoyama, T.; Tanaka, H.; Kuroda, S.; Toriumu, K. *Angew. Chem., Int. Ed.* **2005**, *44*, 4164−4168.

(8) Mitsumi, M.; Ueda, H.; Furukawa, K.; Ozawa, Y.; Toriumi, K.; Kurmoo, M. *J. Am. Chem. Soc.* **2008**, *130*, 14102−14104.

(9) (a) Kitagawa, H.; Onodera, N.; Sonoyama, T.; Yamamoto, M.; Fukawa, T.; Mitani, T.; Seto, M.; Maeda, Y. *J. Am. Chem. Soc.* **1999**, *121*, 10068−10080. (b) Mitsumi, M.; Murase, T.; Kishida, H.; Yoshinari, T.; Ozawa, Y.; Toriumi, K.; Sonoyama, T.; Kitagawa, H.; Mitani, T. *J. Am. Chem. Soc.* **2001**, *123*, 11179−11192. (c) Otsubo, K.; Kobayashi, A.; Kitagawa, H.; Hedo, M.; Uwatoko, Y.; Sagayama, H.; Wakabayashi, Y.; Sawa, H. *J. Am. Chem. Soc.* **2006**, *128*, 8140−8141.

(10) Calzolari, A.; Alexandra, S. S.; Zamora, F.; Di Felice, R. *J. Am. Chem. Soc.* **2008**, *130*, 5552−5562.

(11) Hermosa, C.; Álvarez, J. V.; Azani, M.-R.; Gómez-García, C. J.; Fritz, M.; Soler, J. M.; Gómez-Herrero, J.; Gómez-Navarro, C.; Zanora, F. *Nat. Commun.* **2013**, *4*, 1709−1−6.

(12) Hu, W.; Liu, Y.; Withers, R. L.; Frankcombe, T. J.; Norén, L.; Snashall, A.; Kitchin, M.; Smith, P.; Gong, B.; Chen, H.; Schiemer, J.; Brink, F.; Wong-Leung, J. *Nat. Mater.* **2013**, *12*, 821−826.

(13) Miyasaka, H. *Acc. Chem. Res.* **2013**, *46*, 248−257.

(14) (a) Miyasaka, H.; Campos-Fernández, C. S.; Clérac, R.; Dunbar, K. R. *Angew. Chem., Int. Ed.* **2000**, *39*, 3831−3835. (b) Miyasaka, H.; Izawa, T.; Takahashi, N.; Yamashita, M.; Dunbar, K. R. *J. Am. Chem. Soc.* **2006**, *128*, 11358−11359. (c) Motokawa, N.; Oyama, T.; Matsunaga, S.; Miyasaka, H.; Sugimoto, K.; Yamashita, M.; Lopez, N.; Dunbar, K. R. *Dalton Trans.* **2008**, 4099−4102. (d) Motokawa, N.; Miyasaka, H.; Yamashita, M.; Dunbar, K. R. *Angew. Chem., Int. Ed.* **2008**, *47*, 7760−7763. (e) Motokawa, N.; Oyama, T.; Matsunaga, S.; Miyasaka, H.; Yamashita, M.; Dunbar, K. R. *CrystEngComm* **2009**, *11*, 2121−2030. (f) Miyasaka, H.; Motokawa, N.; Matsunaga, S.; Yamashita, M.; Sugimoto, K.; Mori, T.; Toyota, N.; Dunbar, K. R. *J. Am. Chem. Soc.* **2010**, *132*, 1532−1544. (g) Miyasaka, H.; Morita, T.; Yamashita, M. *Chem. Commun.* **2011**, *47*, 271−273. (h) Miyasaka, H.; Motokawa, N.; Chiyo, T.; Takemura, M.; Yamashita, M.; Sagayama, H.; Arima, T. *J. Am. Chem. Soc.* **2011**, *133*, 5338−5345. (i) Nakabayashi, K.; Nishio, M.; Kubo, K.; Kosaka, W.; Miyasaka, H. *Dalton Trans.* **2012**, *41*, 6072−6074.

(15) Cole, K.; Cole, R. H. *J. Chem. Phys.* **1941**, *9*, 341−351.